JOURNAL OF SPACECRAFT AND ROCKETS
Vol. 38, No. 4, July–August 2001

Critical Design Issues for Airbreathing Hypersonic Waverider Missiles

Ryan P. Starkey* and Mark J. Lewis†
University of Maryland, College Park, Maryland 20742

Tradeoffs involved in the design of a hydrocarbon-fueled, hypersonic waverider-based missile were explored. The problem of providing acceptable vehicle performance in a volume-constrained package was addressed. The specific case of a missile constrained to fit within a 0.61 × 0.61 × 4.27 m naval vertical launch tube was examined, and a parametric study was performed to determine the probabilistic boundaries of designing a Mach 6 missile to satisfy the desired mission goal of a 750-km cruising range. All missile designs were assumed to reach cruising altitude and velocity through the use of an external rocket booster. The key design elements investigated are fuel volume fraction, engine inlet pressure, the number of scramjet engines, and the effects of changing the engine mixing and burning efficiencies. Missile designs were optimized for steady-state trim conditions at the beginning of cruise using genetic algorithm software. The sensitivities of the modeling assumptions on the performance of the final optimized designs are explained. The overall contribution of the optimized designs along with the predicted change in performance expected with increased modeling accuracy allows upper performance and range limits to be established. Double-engine designs are shown to be more promising than single-engine designs for achieving the desired 750-km range, as well as allowing for increased payload.

Nomenclature

A, B, C, D	=	geometric variables
a	=	acceleration, m/s^2
D	=	drag, N
f	=	fuel-to-air mixture ratio
g	=	gravity, m/s^2
h	=	height, m
I_{sp}	=	specific impulse, s
I_y	=	mass moment of inertia, kg-m^2
L	=	lift, N; length, m
M_{C_g}	=	moment about the center of gravity, N-m
m	=	mass, kg
$\dot{m}$	=	mass flow rate, kg/s
p	=	pressure, Pa
R	=	range, km
r_{earth}	=	radius of the Earth, m
S	=	area, m^2
T	=	thrust, N
t	=	plate thickness, m
U	=	velocity, m/s
V	=	volume, m^3
W	=	weight, N
w	=	width, m
x	=	streamwise direction
y	=	spanwise direction
Z	=	altitude, km
z	=	vertical direction
β	=	shock angle, deg
δ	=	forebody leading-edge inclination angle, deg
η	=	efficiency
θ	=	forebody centerline angle, deg; nozzle angles, deg
κ	=	fuel volume fraction
π	=	fuel mass fraction
ρ	=	density, kg/m^3
ϕ	=	equivalence ratio
ω	=	angular acceleration, rad/s^2

Subscripts

a	=	air
box	=	box efficiency
C_g	=	center of gravity
cap	=	capture area
cen	=	centrifugal lift
eng	=	engine
f	=	fuel
frontal	=	frontal area
inlet	=	combustor inlet
m	=	fuel mixing and burning efficiency
max	=	maximum
p	=	pressure lift
s	=	structure
st	=	stoichiometric
S_s	=	based on surface area of a sphere
tung	=	tungsten
v	=	viscous drag
x	=	translational direction
w	=	wave drag, wetted surface area
z	=	vertical direction
1, 2	=	pre- and postshock conditions
∞	=	freestream value

Superscripts

m, n	=	forebody power-law exponents

Introduction

THIS paper explores aspects of the design of missile-class hypersonic waveriders. Waveriders (first conceived of by Nonweiler[1] in 1959) are types of vehicles that are designed to have a bow shock attached everywhere to a sharp leading edge. The primary advantages of using a waverider-based vehicle design are 1) delivering a known flowfield to an airbreathing engine, 2) high values of lift-to-drag ratio L/D at high coefficient of lift, and 3) simplified analysis. The high L/D magnitudes are possible because of the high lift generated by containment of compressed air between the lower vehicle surface and an attached leading-edge shock wave. The shock attachment also increases capture efficiency by minimizing flow spillage and pressure leakage and thus allows smaller shock angles for a given mass capture. These waverider attributes have been predicted by theory[2] and validated using both computational[3] and experimental[4] investigations.

Received 26 April 2000; revision received 5 March 2001; accepted for publication 11 March 2001.

*Faculty Research Assistant, Department of Aerospace Engineering; rstarkey@eng.umd.edu. Member AIAA.

†Professor, Department of Aerospace Engineering; lewis@eng.umd.edu. Associate Fellow AIAA.

For a waverider-based missile the box constraints are twofold: the missile must satisfy the internal structural, payload, and fuel constraints while guaranteeing that the external dimensions fall within the highly constrictive boundaries allowed by a vertical launch tube or wing pylon. As already mentioned, the spatial constraint for the naval vertical launch tube is a rectangular box measuring 0.61 × 0.61 × 4.27 m. This external constraint creates an extremely difficult optimization problem in which solutions can only be found through a high degree of accuracy in all aspects of vehicle modeling.

Waveriders have been explored for this missile application because they allow for low-drag vehicles with pressure containment. This pressure containment necessitates fewer compression ramps to produce the required high inlet pressure needed for combustion of hydrocarbon fuel within a short combustor. The desired scramjet inlet pressure and temperature are provided to the engine(s) through a series of three inlet ramps following a wedge-derived, power-law shaped forebody.[5] These ramps provide the flow to one or more rectangular cross-section scramjet engines, which then exhaust to simple nozzles with contours derived from second-order polynomials.

Because of the highly constrained nature of this design and the difficultly finding feasible designs to initialize a gradient-based optimization, a genetic algorithm approach has been utilized. The optimizations were performed using the genetic algorithm package Implicit Multiobjective PaRameter Optimization Via Evolution (IMPROVE v2.4) developed by Anderson[6] and Anderson et al.[7] The missile geometries are optimized for maximum cruise range while ensuring steady-state trim conditions: thrust equal to drag ($T/D = 1$), lift equal to weight ($L/W = 1$), and zero pitching moment about the center of gravity ($\sum M_{C_g} = 0$). The cruise range was evaluated using the simple Breguet range equation at a single design point. Details on the genetic algorithm methodology and missile performance evaluation are provided.

Design Requirements

Because of the fixed spatial constraints of naval vertical launch tubes, the resulting design of this missile must fall within these geometric boundaries. All missiles presented here utilize the entire length and width allotted with only the height varying between designs. These box dimensions result in a maximum available volume $V_{\max}$ of 1.59 m^3. An implicit goal of this optimization was to fill the constraint box as much as possible to allow for maximum mass (structural, payload, and fuel). Maximizing the vehicle mass enables the designer to take advantage of the high lift offered by waverider geometries, while also maximizing the potential for increased missile range (caused by the increased fuel volume). An increase in volume usually comes at the expense of increased drag (both wave and viscous), which places higher demands on the propulsion system and aerodynamic efficiency, causing increased fuel consumption.

By its nature a waverider-based forebody is assumed to have an infinitely sharp leading edge for shock attachment. In practice, some leading-edge blunting will be needed for both manufacturing and leading-edge cooling requirements. Until recently, the materials necessary for small radius leading edges (required to maintain a waverider flowfield) were nonexistent. The reality of nonablating, extremely sharp leading edges (1-mm radius or smaller) have been achieved in the Slender Hypervelocity Aerothermodynamic Research Probes program at NASA Ames Research Center.[8] The small radius leading edges are made possible through the use of ultra-high-temperature ceramics (UHTCs), such as zirconium diboride and hafnium diboride composites. Research by Ames shows that sustained Mach 7 sea-level flight is achievable without ablation using a sharp UHTC leading edge. These maximum UHTC flight conditions are more severe than those of this missile application. For cases in which some leading-edge blunting is required to reduce local heating to an acceptable level for sustained flight, it has been shown experientially by Gillum and Lewis[9] that minimal flowfield degradation occurs at Mach 14 (<20% change in L/D at $L/D_{\max}$) for a 6.3-mm-radius leading edge on a 0.99-m-long, 0.41-m-wide waverider (i.e., relatively large leading-edge blunting).

Tarpley and Lewis[10] showed that optimizing a waverider-based vehicle and then sizing the control surfaces required for trimmed flight could result in undesirable magnitudes of restoring control forces and increased drag by as much as 100%. Considerable performance improvements can be achieved by including the vehicle trim (at zero angle of attack) as a constraint of the optimization process. As such, this methodology, originally developed for manned cruise vehicles, has been successfully reproduced here.

All missiles were optimized for the steady-state trim conditions $L = W$, $T = D$, and $\sum M_{C_g} = 0$. Because a simple Breguet approximation was used to determine cruise range, trajectory considerations were neglected. Also, because of complications associated with analyzing off-design conditions (i.e., for nonzero angles of attack), only zero angle of attack has been investigated. This was done to avoid problems associated with forebody and airframe flow spillage (highly three-dimensional flowfields) and shock/shock and/or shock/expansion-fan interactions on the inlet and within the combustor. This simplification was deemed acceptable based on the range approximation used and the results desired. Because all missiles were evaluated only at zero angle of attack, pitching moment was trimmed solely through control surface deflections.

Takashima and Lewis[11] found that optimizing a vehicle for its cruise conditions provided a nonoptimal design from an overall mission perspective. Therefore, it is clear that the vehicles designed in this study were not truly range optimized, rather, they were used as a first-order investigation to determine the possible advantages achievable by different inlet conditions, engine quantity, fuel volume fraction, and combustor mixing and burning efficiency.

Missile Model

Optimized missile configurations are shown in Figs. 1–7. These figures can be referred to for clarity throughout the modeling section, and further discussion of these missile geometries are included in the Results section.

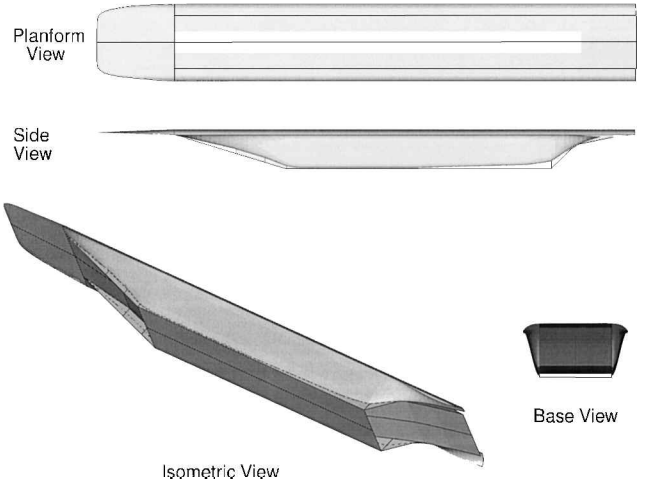

Fig. 1 Case 1: $p_{\text{inlet}} = 8$ atm, $\kappa = 30\%$, $\eta_m = 50\%$.

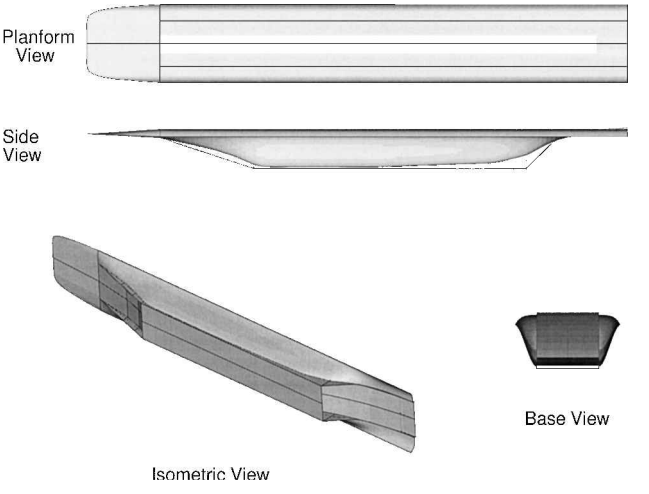

Fig. 2 Case 2: $p_{\text{inlet}} = 8$ atm, $\kappa = 30\%$, $\eta_m = 100\%$.

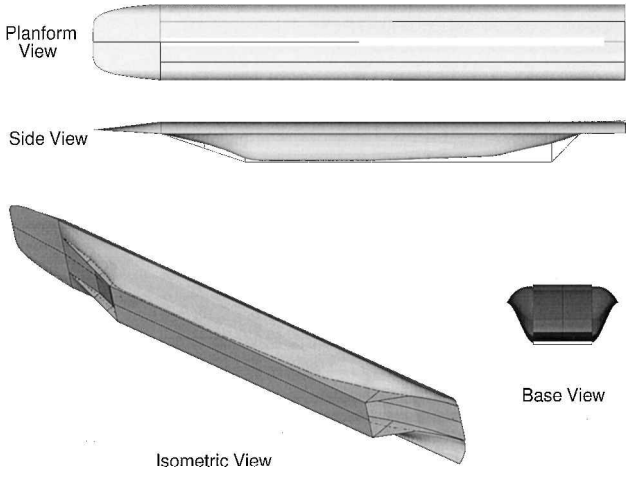

Fig. 3 Case 3: $p_{inlet} = 8$ atm, $\kappa = 50\%$, $\eta_m = 100\%$.

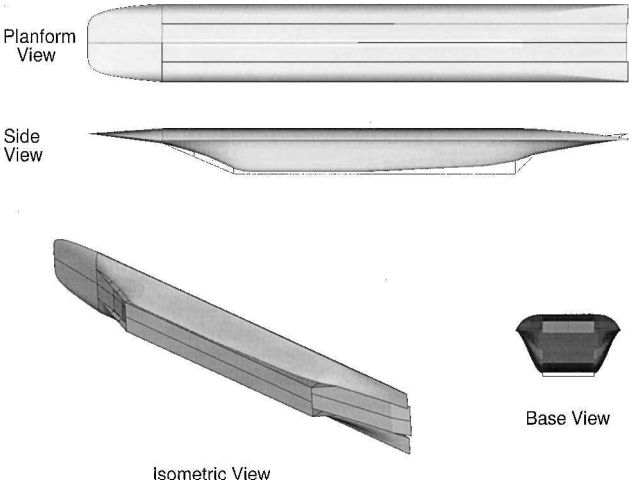

Fig. 4 Case 4: $p_{inlet} = 4$ atm, κ,= 50%, $\eta_m = 100\%$.

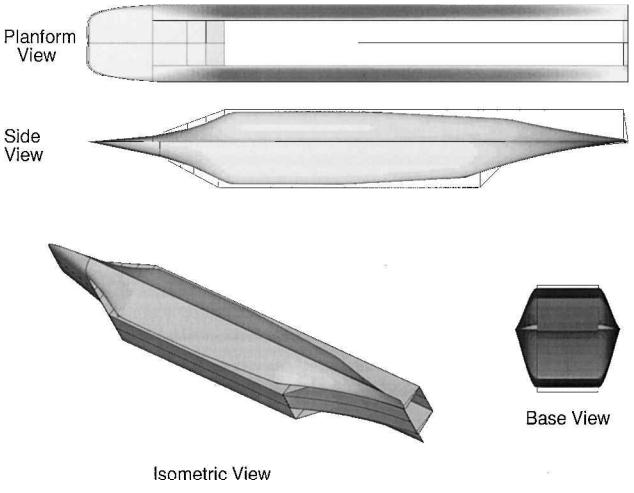

Fig. 5 Case 5: $p_{inlet} = 8$ atm, $\kappa = 30\%$, $\eta_m = 100\%$.

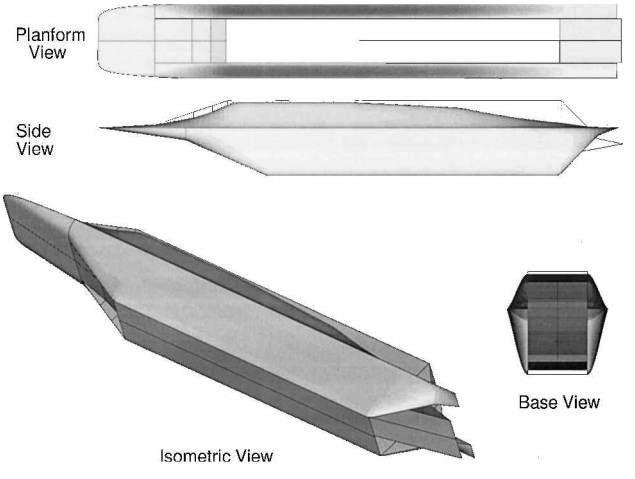

Fig. 6 Case 6: $p_{inlet} = 8$ atm, $\kappa = 50\%$, $\eta_m = 50\%$.

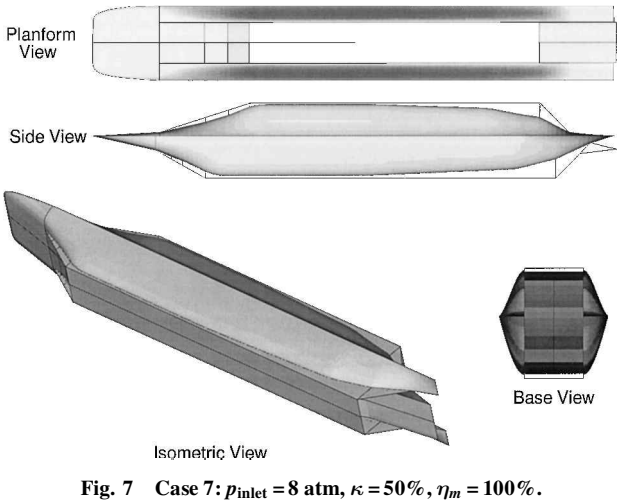

Fig. 7 Case 7: $p_{inlet} = 8$ atm, $\kappa = 50\%$, $\eta_m = 100\%$.

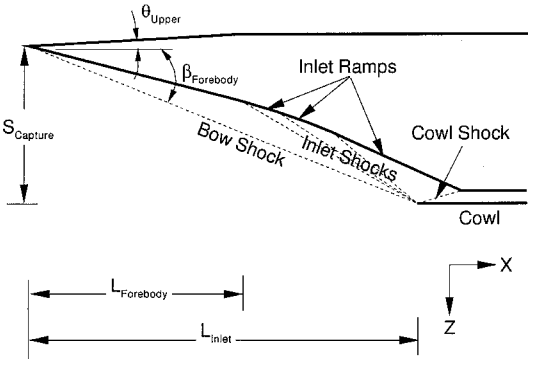

Fig. 8 Inlet geometry and shock system along the keel line for a single engine missile.

Forebody

Exceptionally large inlet pressure was required for this missile to combust a hydrocarbon fuel without additives (see Scramjet section for details). A waverider-based forebody provided an ideal solution. Waverider forebodies minimize pressure leakage between upper and lower inlets (depending on the configuration and number of engines), thereby maximizing the mass flow captured by the engine(s). In addition to the leading-edge shock attachment requirement, the forebody was further constrained to provide a planar section and associated planar shock for the width of the engine to ensure shock attachment with the cowl lip (on design condition) of a rectangular engine. Under these conditions, the cowl shock was subsequently canceled at a corner just downstream of the inlet to the engine. An example of the forebody/inlet geometry and shock arrangement along the keel line for a single engine missile is shown in Fig. 8.

By restricting the forebody and inlet system to produce a planar flowfield, many of the problems associated with three-dimensional nonplanar flowfields have been avoided. Not only is a three-dimensional flowfield much more difficult to analyze and more computationally expensive, but boundary-layer growth will be quicker, and separation will occur more readily. In addition, the flow spillage associated with three-dimensional flow would lower the mass flow rate (and inlet pressure) into the combustor and alter the mixing

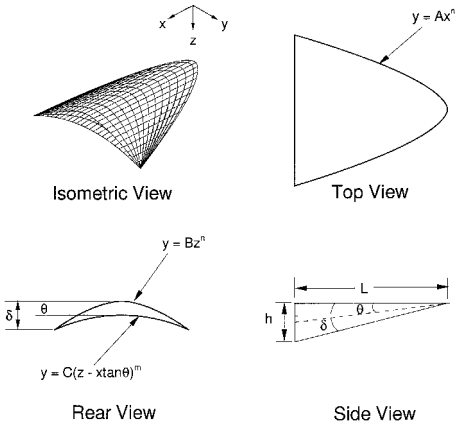

Fig. 9 Example waverider forebody generated using the variable wedge angle method.

effects and mixing profile. Clearly, these are complex issues and flow phenomena, which should be avoided if possible.

Waverider forebodies were generated using the analytical Variable Wedge Angle (VWA) method, which was derived and validated in previous works.[5,12] The VWA method uses three power-law equations [$y = Ax^n$, $y = Bz^n$, and $y = C(z - x\tan\theta)^m$] to geometrically define the forebodies, as shown in the example in Fig. 9. For the purposes of this paper, the forebody utilized a constant wedge angle at each spanwise location to provide uniform flow into the scramjet engine. Although the waverider surface is two-dimensional for the width of the engine, this model generates configurations with three-dimensional shock structures.

Because of the large amounts of lift generated by the waverider forebodies, resulting moments and net lift of single-engine designs were often too large for the optimizer to find trimmed solutions. This deficiency was overcome by allowing the upper surface of single-engine configurations to generate compression, thereby mitigating undesirable lift and moment difficulties. This compression surface was represented by θ_{upper} in Fig. 8. Multiple-engine configurations did not encounter these problems because they have counteracting (generally nonsymmetric) forebody compression surfaces.

Inlet

The inlet for this missile uses three successive compression ramps (for each engine) in addition to the forebody compression. The inclination angle of the three compression ramps following the forebody was constrained to have at least the same shock jump pressure ratio as the previous ramp (i.e., increasing local wedge inclination angle). The inlet was designed so that the shocks from the forebody, as well as the three compression ramps, all converge at the cowl lip (as was shown in Fig. 8). Although this shock-on-lip condition was not optimal from a thermal standpoint, the condition provides the maximum mass flow to enter the engine.

The inlet ramps were set to be the same width as the engine. Inlet length was set implicitly by shock-on-lip conditions for all inlet shocks. Therefore, the inlet geometry directly defines the engine dimensions, inlet properties, and mass flow rates. Scramjet inlet pressure and temperature requirements were used to determine the three compression ramp angles and the cruising altitude once the forebody compression angle has been selected. As can be seen in the optimized missiles shown in Figs. 1–7, the inlet system utilized thin sidewalls to aid in preventing flow spillage, thereby maximizing airflow into the engines.

Conical inlets were not considered in this study for a number of reasons. First, the high inlet pressures (8 atm) would require a long, large-diameter, multiple-ramp conical inlet. Not only would this geometry exceed the imposed box constraints (for maximum mass flow, shock-on-lip condition), but would also create an inlet with nonuniform flow properties entering the combustor. Second, a purely conical missile would need to operate at angle of attack to generate the lift necessary to offset weight. This off-design condition would create more difficulties analyzing flowfield nonuniformities than desired for the straightforward analytical model generated for this study. Third, handling side compression and shock effects created by struts in a circular scramjet combustor was outside the scope of a simple analytical model. Finally, utilizing a conical inlet would necessitate the use of both an axisymmetric scramjet (to maximize mass flow) and a axisymmetric nozzle. Clearly, an axisymmetric missile with a conical inlet system is a completely different problem, which was thought to result in a less efficient vehicle while having a much more difficult flowfield to analyze. Therefore, only missile configurations with planar inlets and rectangular scramjets were analyzed in this study.

Scramjet

Hydrocarbon fuels offer many desirable properties for this vehicle scale, such as high mass density and straightforward handling requirements. However, the problem arises of how to get the hydrocarbon fuel to mix and burn in a shorter combustor than is normally associated with hydrogen burning scramjets. Possible solutions are to use high inlet pressure and temperature and/or adding a piloting agent (i.e., silane).

Inlet pressure was one of the critical design requirements in this study. Preliminary investigations[13] have shown that complete burning of JP-7 fuel with 10% silane (by mass flow rate of oxygen) can be achieved in about 1.2 m using an inlet pressure and temperature of 8 atm and 1200 K, respectively. The silane needed for combustion at these inlet conditions introduces undesirable fuel-handling complications and operational restrictions. Because the need for silane was not desirable, all possible opportunities to eliminate its use are being explored. For the purposes of this study, the combustor inlet pressure was varied between 4 and 8 atm. This pressure variation was performed to determine the possible benefits achievable by using a lower inlet pressure (with the definite need for a silane pilot), as compared to the higher pressure inlet where the need for silane could be eliminated by extending the minimum combustor length to 1.8 m.

A hydrocarbon-fueled scramjet was assumed with normal injection, calculated using Shapiro's influence coefficients.[14] Boundary-layer effects in the engine were determined using momentum deficit accounting. Heat release caused by combustion was modeled using an assumed exponential total temperature profile. The fuel mass flow rate $\dot{m}_f$ was determined by the optimizer and therefore varies for each vehicle configuration and each engine. The temperature within the engine was constrained from exceeding an imposed material limit of 2500 K, but this limit was rarely encountered.

The combustor was designed to have a constant area for half of the length and to have a diverging section for the remaining half. The angle of the diverging section was held constant at 3 deg. This diverging section allows the engine inlet height to be smaller by allowing additional heat to be released in the diverging section while allowing an area increase to avoid thermal choking.

Nozzle

The nozzle length and height were implicitly constrained because of the overall dimensional restrictions of the missile. Once the inlet and combustor dimensions have been determined, the remaining length and height were assigned to the nozzle. This results in a nonideal nozzle geometry, which could develop a complex flowfield containing multiple expansion/compression waves inside the nozzle. The nozzle expansion angle was constrained such that the resulting nozzle wall geometry will always be concave (to avoid flow separation). The nozzle flowfield was calculated using the two-dimensional method of characteristics.[15] The nozzle was defined such that there was an internal nozzle followed by an external half plug nozzle, as shown in Fig. 10. A second-order polynomial curve fit ($z = Ax^2 + Bx + C$) was used to define the nozzle wall.

A portion of the trailing edge of the nozzle was used as a control surface. This feature can be incorporated with little impact on propulsion performance because the pressures at this point are relatively low and contribute little to the thrust of the vehicle (i.e., primarily lifting forces). In addition, the nozzle portion was chosen for the control surface because it was desired to have few moving parts on the missile, thereby eliminating the option of deployable control surfaces.

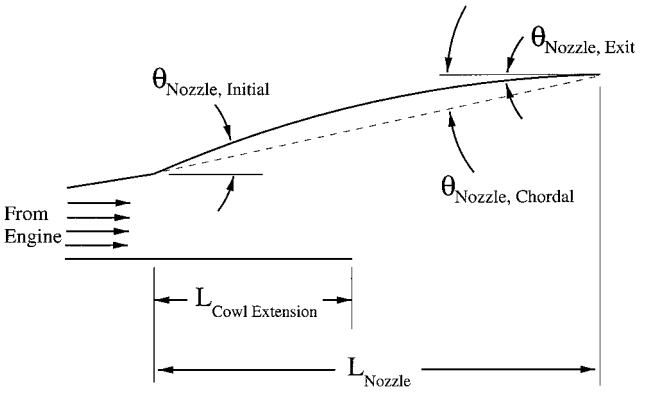

Fig. 10 Nozzle design variables.

Airframe

All aerodynamic parameters for the airframe were calculated using shock-expansion theory,[16] using oblique shock relations and Prandtl–Meyer expansion theory. The vehicle model used in this study assumes that the flow runs straight back along the vehicle surface (i.e., no transverse flow). This assumption will tend to overpredict pressures for highly curved surfaces, as encountered near the forebody/aftbody transition region, particularly in double-engine configurations. The double-engine missile designs had much blunter forebodies (i.e., more compression) with more transverse curvature than the single-engine designs. The added bluntness in the double-engine missiles was required to meet the desired inlet conditions within the constraints imposed by the vertical launch tube. The larger curvature results from the fact that the double-engine configurations generally have wider combustors to maximize capture area, thereby leaving less room for the airframe. These bluntness and curvature effects can been seen in the optimized missiles in Figs. 1–7. This pressure overprediction was thought to be an acceptable modeling deficiency for the current designs because it places higher demands on the propulsion system helping to balance any optimistic engine assumptions.

The aftbody uses third-order polynomial curve fits ($z = Ay^3 + By^2 + Cy + D$) at each streamwise location by matching the slope of the keel line to a leading edge, which was oriented parallel to the freestream at zero angle of attack. The upper/lower-surface attachment angle was allowed to vary in the streamwise direction to keep a smooth profile along the aftbody. The maximum upper/lower-surface attachment angle was also permitted to vary among designs. The keel-line attachment point can vary through any position along the combustor side wall. These variations allow for volume (and force) manipulation where needed during the optimization process.

Viscous Effects

Viscous drag for this model was calculated using the reference temperature method[17] with Eckert's empirical estimate for the average boundary-layer temperature. To keep this model simple, a single estimate for the wall temperature (1200 K) was used over the entire vehicle. This wall temperature is a reasonable approximation for hypersonic vehicles at cruise conditions assuming active wall cooling. The flow was assumed to be entirely turbulent to overpredict any viscous drag, thereby helping counteract any optimistic propulsion assumptions. Dynamic viscosity at the reference temperature was approximated by Sutherland's law.[17] No detailed heat-transfer or thermal protection system analyses were performed.

Structure

Although a detailed mass distribution and composition have not been performed for this analysis, some reasonable approximations have been made. The missile was assumed to have some usable fuel volume fraction κ of the interior volume V, with a high-density tungsten shell ($\rho_{\text{tung}} = 19{,}255\ \text{kg/m}^3$) with a plate thickness of 6.35 mm. This thick tungsten shell was used to approximate the mass of all missile subsystems and structural components (i.e., everything other than fuel). Using JP-7 fuel ($\rho_f = 940\ \text{kg/m}^3$) results in an approximate missile weight of

$$W = g[S_w\, t_{\text{tung}}\, (\rho_{\text{tung}} - \kappa\rho_f) + \kappa V \rho_f] \tag{1}$$

The value of κ was one of the critical design parameters under investigation in this study. Cases were examined with values of κ of either 30 or 50%. This parameter was important because 1) different configurations have different usable volumes and 2) as volume is increased the individual volumes of the payload, avionics, pumps, etc. should remain relatively constant (thereby allowing more useful volume for fuel).

Tungsten was chosen because of its large density to aid in negating excessive lift generated by the forebody in single-engine configurations and to provide kinetic energy at impact for enhanced missile lethality. Large structural mass is actually beneficial for the aerodynamic performance of single-engine cases but detrimental to the double-engine designs that can effectively reduce lift by offsetting engines (excess mass places undue lift requirements on the lower section).

This simple model has practical limits. Assuming that all of the mass is confined to a shell around a constant density core (fuel), the moment of inertia becomes artificially high requiring large geometric adjustments to negate the moment during optimization (i.e., providing trim to counteract unrealistic moments). In addition, without a realistic structural model the effects of fuel loss, payload size and density, usable volume, thermal requirements, and subsystem size, density, and placement cannot be thoroughly assessed.

Figures of Merit

For purpose of analysis and comparison of different results, a number of different figures of merit were used. Although the performance and design of a hypersonic vehicle of this scale is an extremely complex problem, because of the highly coupled performance relationships figures of merit can be grouped into the subsystems on which they have the most noticeable impact.

Engine Analysis

Specific impulse I_{sp} is a measure of the amount of thrust generated for a given weight flow rate of fuel:

$$I_{\text{sp}} = T/\dot{m}_f g \tag{2}$$

The mass flow rate of fuel added to the available mass flow rate of air $\dot{m}_a$ is described by the fuel mass fraction f. By relating this to the amount of fuel needed to burn all of the oxygen (i.e., stoichiometric combustion) f_{st}, the equivalence ratio ϕ is defined by

$$\phi = \frac{f}{f_{\text{st}}} = \frac{\dot{m}_f/\dot{m}_a}{(\dot{m}_f/\dot{m}_a)_{\text{st}}} \tag{3}$$

This figure of merit tells how fuel lean the combustors are running (i.e., $\phi < 1$). For the JP-7 fuel used in this study, $f_{\text{st}} \approx 0.0671$.

Mixing and burning efficiency η_m is related to the energy recovery from the fuel added. It is an assumed efficiency parameter to relate the unknown effects of the inlet pressure and temperature to the fuel mixing and burning lengths, mixing efficiency, and the effects of expansion (both internal to the engine and the nozzle) on equilibrium chemistry assumptions. Therefore, when determining the total temperature rise that is possible for a given amount of fuel addition, the efficiency parameter simply lets unburned fuel mass pass through the combustor. To attempt to bracket the results that can exist in a real engine of this type and also to account for the already mentioned unknown parameters, values of both 50% and 100% were examined for η_m.

Geometric Analysis

For the purposes of determining volumetric efficiency, a comparison was made to a sphere of equal volume (surface area comparison) because a sphere is the most volumetrically efficient shape possible, resulting in

$$\eta_{S_s} = (36 \times 3.1415927)^{\frac{1}{3}} V^{\frac{2}{3}} \Big/ S_w \tag{4}$$

As already mentioned, an important volumetric parameter for this missile application was how well the design fills the available box size. Filling the design volume as much as possible should aid in maximizing the missile range. This goal results in a volumetric efficiency figure of merit based on box size:

$$\eta_{\text{box}} = V/V_{\text{box}} = V/1.59\,\text{m}^3 \tag{5}$$

For the vehicles studied the volume used was the structural and internal volume. The volume internal to the scramjet engines was assumed to be lost and was not included in these figures.

The amount of airflow processed by each engine was related through a capture-area efficiency:

$$\eta_{\text{cap}} = S_{\text{cap}}/S_{\text{frontal}} = S_{\text{cap}}\Big/0.372\,\text{m}^2 \tag{6}$$

where S_{frontal} is the total available frontal area of the box [i.e., $(0.61\ \text{m})^2$]. Obviously, increased capture efficiency allows for a larger percentage of the available mass flow to pass into the combustors. Because this analysis was only concerned with zero angle-of-attack flight, the maximum capture area available is the frontal projected area of the box.

Another geometric figure of merit is the fuel mass fraction π_f:

$$\pi_f = m_f/(m_f + m_s) \tag{7}$$

For a vehicle of this scale, it was assumed that π_f would never realistically exceed about 0.20. For a single design increasing the fuel mass fraction would increase the vehicle range.

Aerodynamic Analysis

The most common aerodynamic figure of merit is the L/D, which was used to assess the aerodynamic efficiency of the vehicle:

$$\frac{L}{D} = \frac{L_p + L_{\text{cen}}}{D_w + D_v} \tag{8}$$

The centrifugal component of lift L_{cen} is given by

$$L_{\text{cen}} = m\,U^2\Big/(r_{\text{earth}} + Z) \tag{9}$$

where the total missile mass m is $m_f + m_s$ and the radius of the Earth r_{earth} is 6357 km.

Optimization

The design constraints placed on this missile create interesting optimization challenges. As would be expected for waverider-based hypersonic missiles, the component forces were an order of magnitude larger than the net forces (i.e., total positive and negative lifting forces can both be on the order of 10 times the vehicle weight). Another challenge in obtaining an optimized design is remaining within the actual physical boundaries imposed by the box. Coupling these complications together with a gradient-based optimization package resulted in several practical difficulties; small changes in many of the variables could change the design from an ideal missile configuration to one that was unrealistic or simply was not geometrically feasible. These sensitivities created problems with an optimizer that must spend a large part of its time in a viable design space. A genetic algorithm optimization methodology was used to overcome these optimization obstacles.

A Pareto-based evolutionary optimization with exponential apportioning was performed using the shareware code IMPROVE.[6] In the simplest sense a genetic algorithm (GA) is a random number based trial-and-error approach to optimization. A GA does not need an initial guess to begin the process, rather it starts with a population of initial solutions and then selects the best performers to survive and then reproduce. Once an entire generation of solutions have been evaluated, the GA looks at the statistics for the entire population and then determines the survivors through a tournament selection process (i.e., randomly picking chromosomes where the ones with better overall performance for the objective functions were selected). After the tournament the survivors were allowed to crossover and mutate to determine the offspring. Multiple objective functions were solved for simultaneously, and the relative performance of each was determined using an exponential decrement weighting system. This feature allows for the most critical design objective to be given the highest priority when determining the fittest chromosomes for reproduction. Details on genetic algorithms can be found in many texts.[18,19]

Design Variables and Constraints

There were 15 design parameters used for the single-engine cases and 19 used for the two-engine cases. The only nongeometric parameters in the optimizations were the fuel equivalence ratios (one for each engine). The desired parameter resolutions dictate a chromosome length of 72 genes for the single-engine design case. The number of possible designs out of this set of variables was therefore 2^{72} or approximately 10^{21} combinations. In the two-engine configurations the chromosome lengths increase to 95 ($\approx 10^{28}$ combinations). The shear magnitude of possible combinations makes for a challenging programming problem to ensure the vehicle design code was robust enough to consider many different and infeasible situations. The optimized vehicles presented in this study required between 60,000 to 120,000 function calls to converge (i.e., each function call is one vehicle design) and consumed between 12 and 24 CPU hours each on a 433-MHz DEC Alpha computer.

To restrict the optimizer to acceptable missile configurations, a number of objective functions have been minimized. These conditions provide a restrictive boundary on the region of feasible design conditions:

1) Translational acceleration a_x: Because no trajectory analysis was included in this present work, thrust is set equal to drag at the beginning of the cruise altitude (i.e., zero angle of attack):

$$a_x = (T - D_w - D_v)/m \tag{10}$$

2) Vertical acceleration a_z: The net lift at cruise altitude was constrained to be equal to the initial cruising weight of the missile:

$$a_z = (L_p + L_{\text{cen}} - W)/m \tag{11}$$

3) Angular acceleration ω: To achieve a steady-state cruise condition, zero pitching moment about the center of gravity was desired:

$$\omega = \frac{\sum M_{\text{Cg}}}{I_y} \tag{12}$$

4) Cruise range R: The optimization objective was to maximize the range of the missile at cruise altitude using the Breguet range equation assuming that no fuel has been used in reaching cruise altitude:

$$R = U_\infty I_{\text{sp}} \left(\frac{L_p + L_{\text{cen}}}{D_w + D_v}\right) \ell n \left(\frac{m_s + m_f}{m_s}\right) \tag{13}$$

The Breguet range equation assumes a constant value of the vehicle lift-to-drag ratio, which was a reasonable assumption for these very low L/D configurations. The relation provides a simple range evaluation with minimal effort. The minimum desired cruise range for this missile application was 750 km, which would result in an approximate cruising flight time of 7 min at Mach 6. Preliminary studies have indicated that a rocket booster could accelerate these missiles to cruising altitude and velocity in under one minute.

Parametric Study Cases

The parametric study presented varies the magnitudes of the design parameters for which reasonable approximations are unknown, which should help to resolve the bounding box of the feasible design space. Some parameters give undue credit to certain designs, whereas others are a detriment. Therefore, the results of this paper should not be taken as absolutes. Rather, each case should be studied with both the optimistic and pessimistic assumptions which accompanied its design. The study consists of vehicles generated using the combinations of parameters shown in Table 1. The inlet pressure p_{inlet}, fuel volume fraction κ, and fuel mixing and burning efficiency η_m were deemed the most critical design parameters for this study. For cases 1 through 7 converged solutions were achieved

Table 1 Parametric study cases

Case number	No. of engines	p_{inlet}, atm	κ	η_m	Solution found
1	1	8	0.3	0.5	Yes
2	1	8	0.3	1.0	Yes
3	1	8	0.5	1.0	Yes
4	1	4	0.5	1.0	Yes
5	2	8	0.3	1.0	Yes
6	2	8	0.5	0.5	Yes
7	2	8	0.5	1.0	Yes
8	1	4	0.3	1.0	No
9	2	4	0.3	1.0	No
10	2	4	0.5	1.0	No

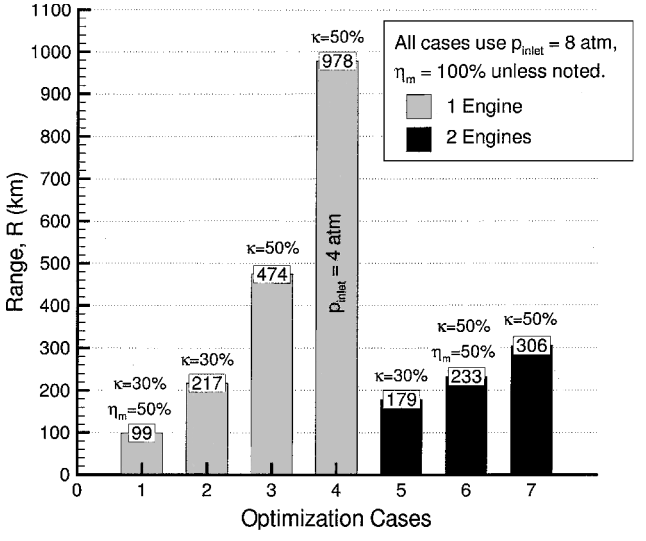

Fig. 11 Range comparison.

for trimmed, steady-state cruise, whereas for cases 8 through 10 converged solutions were not found. The nonconvergence of cases 8 through 10 provides exceptional insight into the design space and will be commented on in the Results section.

Results

The optimized designs for cases 1 through 7 (Table 1) are shown in Figs. 1–7, respectively (flow is from left to right). Some common traits among the different cases are immediately noticeable: 1) nearly identical forebody lengths and planform contours (planar engine flow requirement dictates the spatulate nose shape), 2) single-engine designs trimmed with very little control surface deflection (negative if any), and 3) double-engine designs with $\kappa = 50\%$ (cases 6 and 7) requiring substantial positive control-surface deflections for trim (zero angle of attack). Results of the important figures of merit for each of these cases are shown in Figs. 11–25.

With the ultimate objective of this study being to determine possible design improvements and refinements that would increase the cruising range of a Mach 6 missile, the range results of Fig. 11 are of paramount importance. It is imperative not to interpret them as stand-alone results, as the design conditions lend significantly to the credibility of each result. From this figure it becomes clear that the engine inlet pressure has the largest effect on the missile range, although for this study it was only varied between 4 and 8 atm. Case 4 was the only converged case for $p_{\text{inlet}} = 4$ atm and resulted in about a 100% increase in range over case 3 ($p_{\text{inlet}} = 8$ atm). As already mentioned, operating the hydrocarbon engine at 4 atm inlet pressure would definitely require the addition of silane or some other piloting scheme. This silane requirement, in addition to the fact that case 4 was run with unreasonably high fuel volume fraction ($\kappa = 50\%$) and burning efficiency ($\eta_m = 100\%$), indicates that this particular result would be difficult to implement in actual practice. However, it does effectively demonstrate the dominating influence of the inlet pressure on increasing the range. The most realistic design conditions are somewhere between cases 1 and 2 for the single-engine missiles

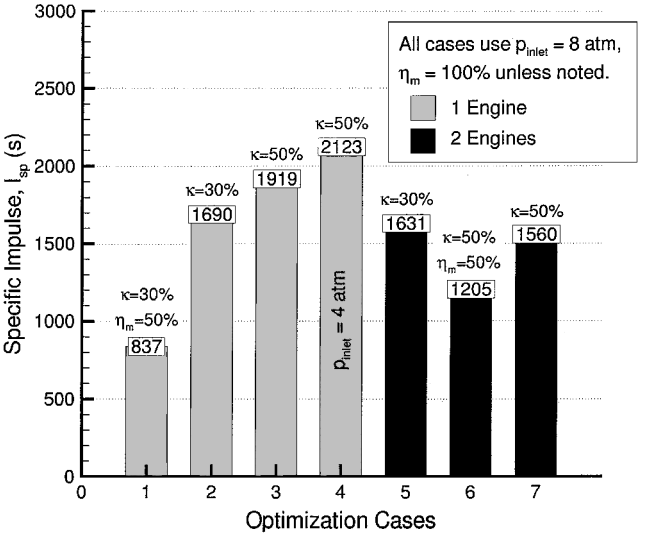

Fig. 12 Specific impulse comparison.

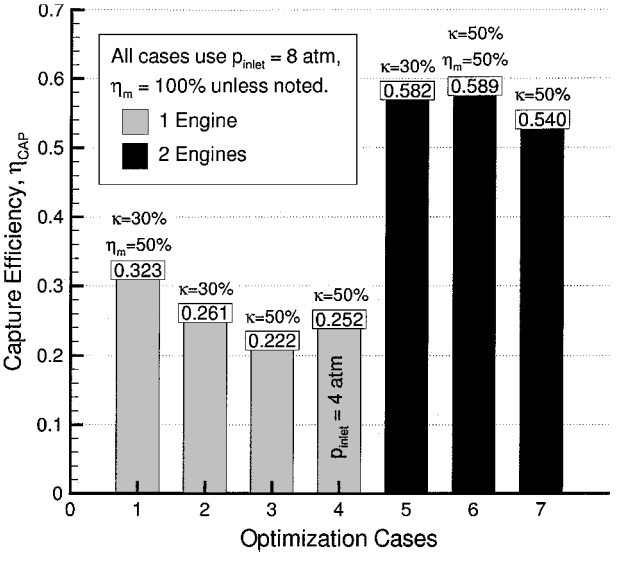

Fig. 13 Capture-area efficiency comparison.

and anywhere between cases 5 through 7 for the double-engine missiles. From the overlap of range for these two regions (cases 1 and 2 and 5–7), no definite conclusion on the supremacy of the single- or double-engine missiles can be made other than the most realistic design conditions favors the two-engine configurations. The case for the double-engine configurations is further strengthened by the fact that they would have larger payload capacity and more kinetic energy than the single-engine designs.

In reviewing Figs. 11–25 it can also be seen that throughout a large number of the figures of merit the two-engine designs were geometrically and aerodynamically limited because of the external box constraint, whereas the single-engine missiles were not. The single-engine designs were all approximately only half the height of the box, with only case 4 ($p_{\text{inlet}} = 4$ atm) exceeding half of the box height. Because of the lower propulsive requirements, the width of the engines for single-engine designs increased in size as needed, whereas the two-engine designs had nearly constant engine widths (Fig. 22). This box limitation was especially noticeable in Fig. 19 (box efficiency), which also translates to the nearly constant value of total drag (Fig. 24) for the two-engine cases.

The various engine parameters in the figures of merit show that the vehicle designs perform as expected, in that as η_m decreases the values of ϕ, $\dot{m}_f$, $\dot{m}_a$, and w_{eng} all increase (as shown in Figs. 14–16 and 22, respectively), and the specific impulse I_{sp} (Fig. 12) decreases as a result of the decreased efficiency. From Fig. 12 it was also evident

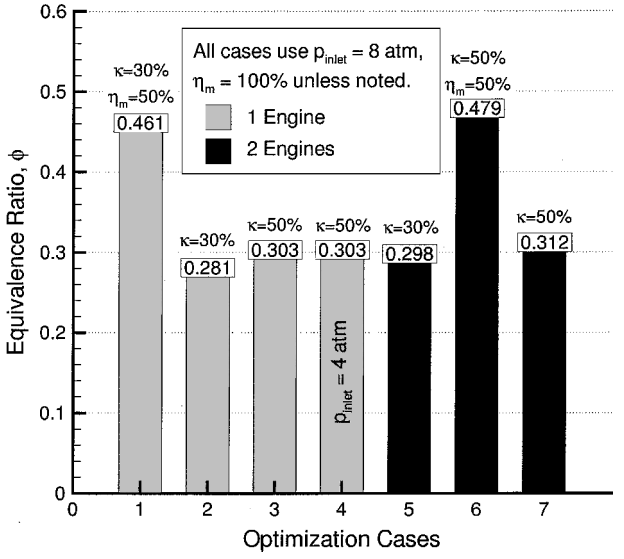

Fig. 14 Equivalence ratio comparison.

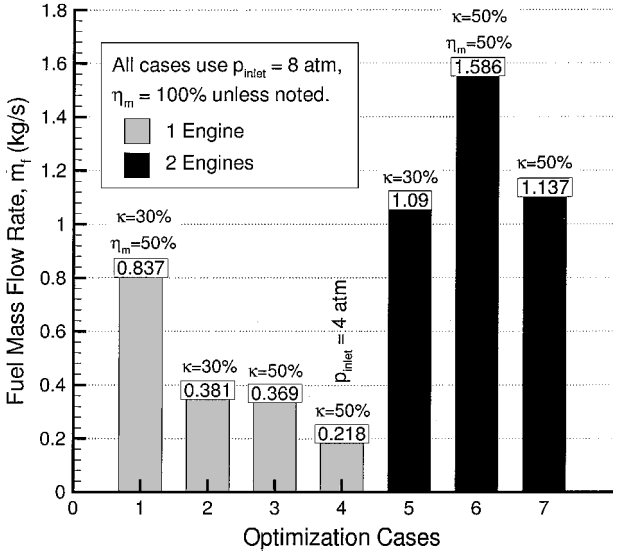

Fig. 15 Fuel mass flow rate comparison.

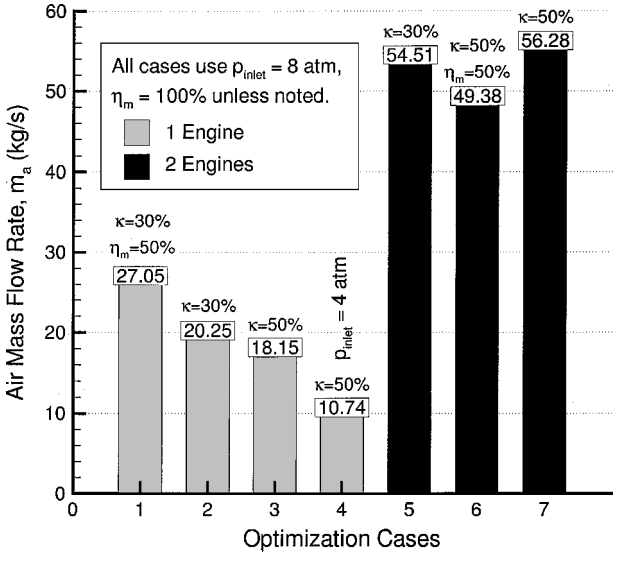

Fig. 16 Air mass flow rate comparison.

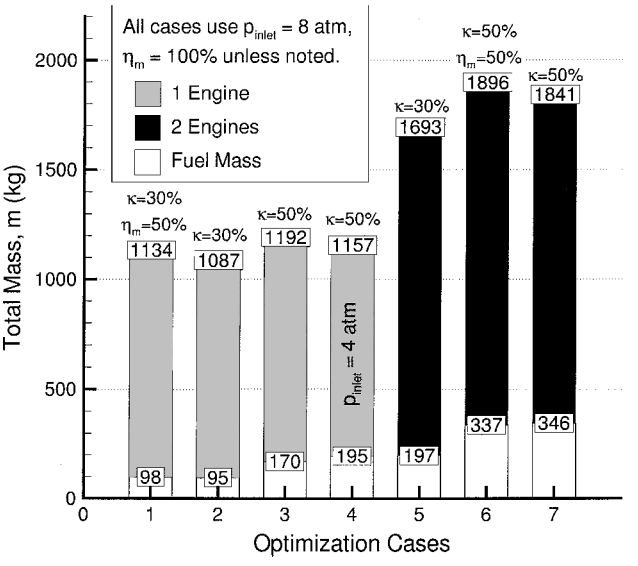

Fig. 17 Mass comparison.

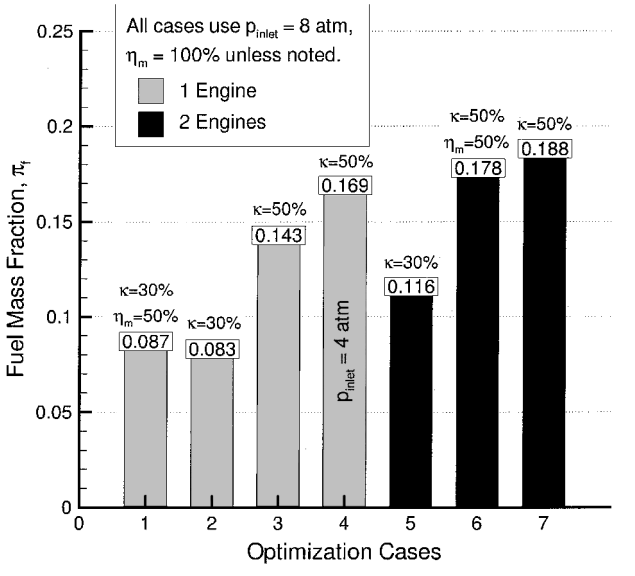

Fig. 18 Fuel mass fraction comparison.

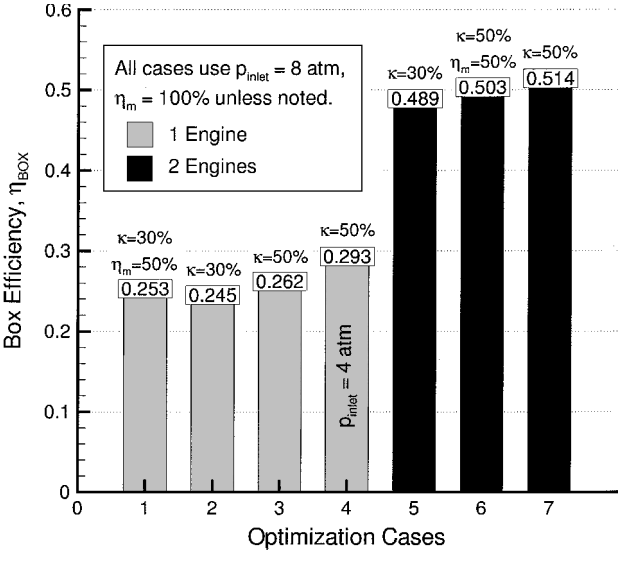

Fig. 19 Box efficiency comparison.

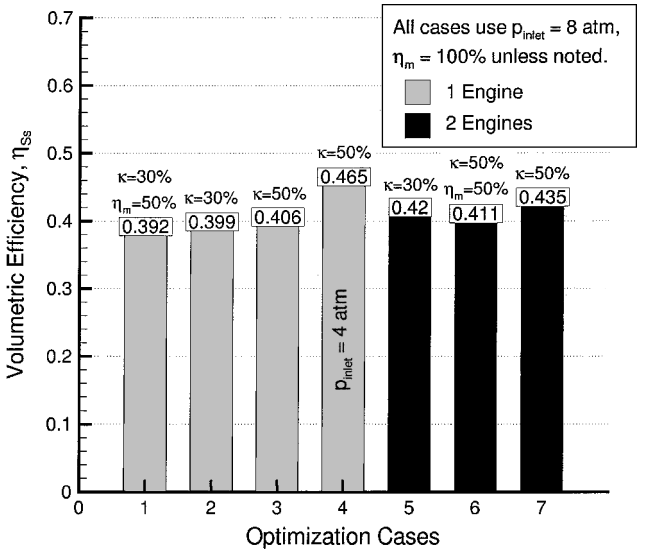

Fig. 20 Volumetric efficiency comparison.

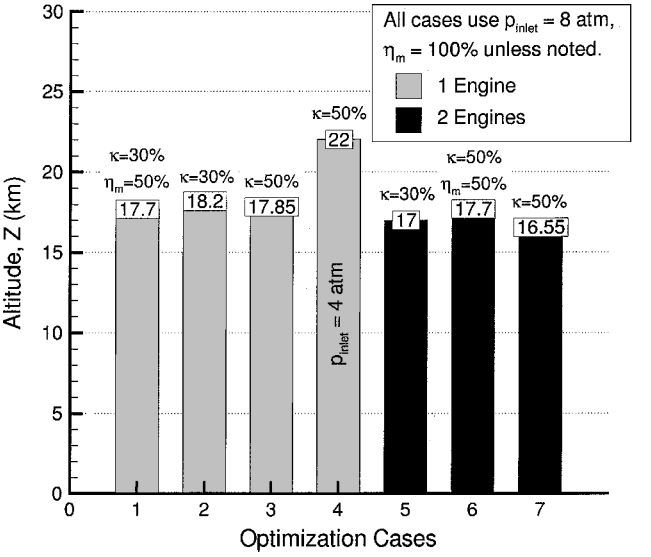

Fig. 23 Altitude comparison.

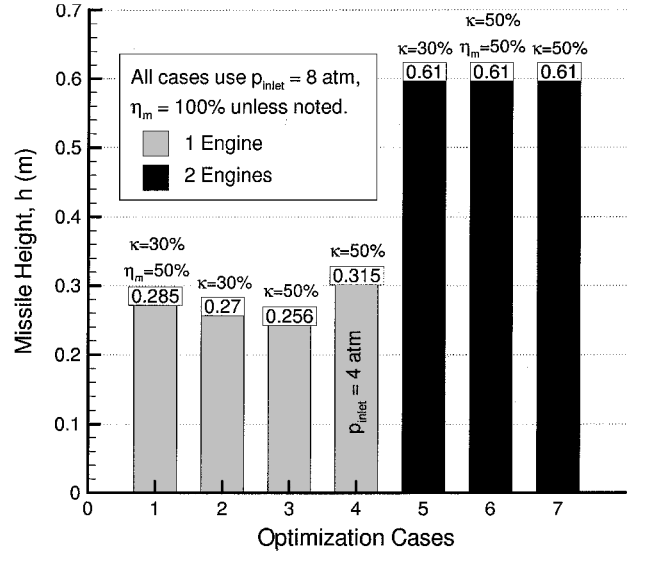

Fig. 21 Height comparison.

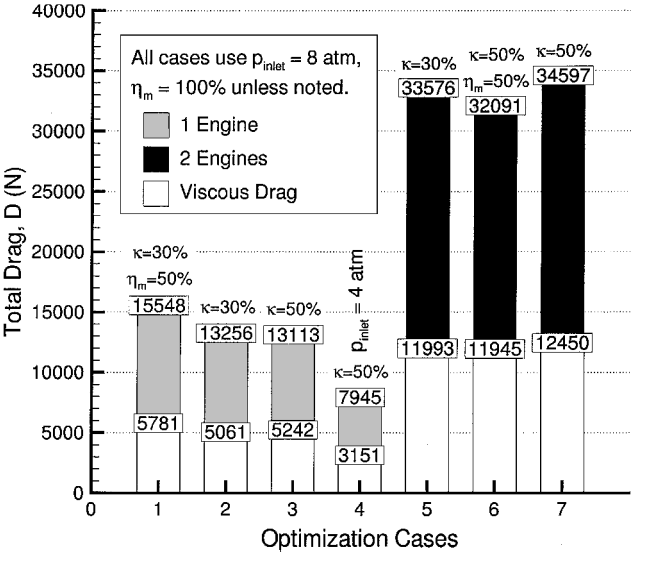

Fig. 24 Drag comparison.

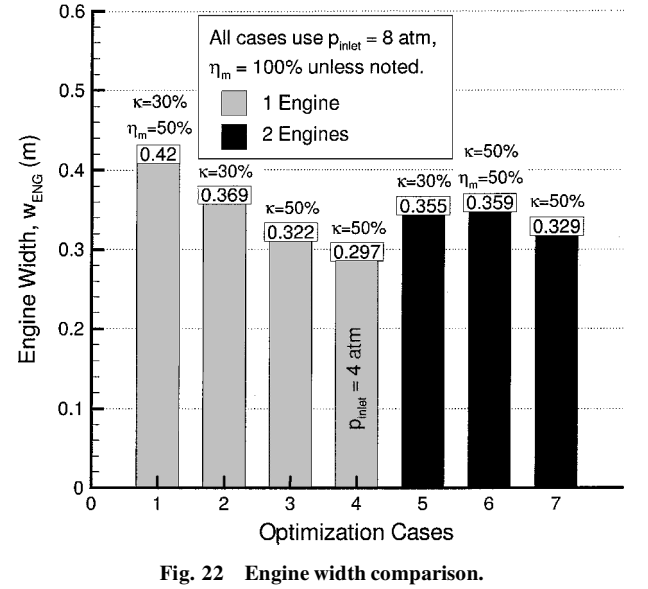

Fig. 22 Engine width comparison.

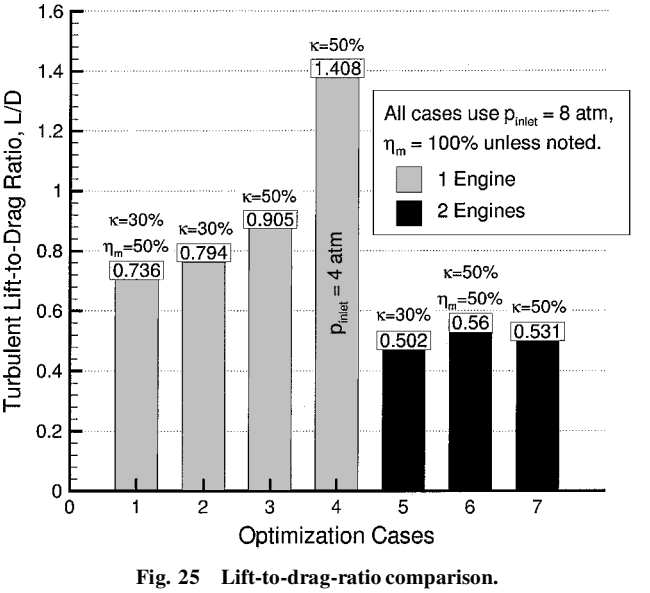

Fig. 25 Lift-to-drag-ratio comparison.

that the engine designs were all very optimistic for $\eta_m = 100\%$. Cases 1 and 6 demonstrate the more typical performance expected of a hydrocarbon-fueled scramjet engine. This overestimation in engine performance allows for a 119% increase in range for the single-engine missiles and a 24% increase for the two-engine case.

Lowering the inlet pressure from 8 atm to only 4 atm on cases 8 through 10 resulted in some surprising conclusions. Figure 23 plots the altitude of each case, showing the large jump from $Z \approx 17$ km for the $p_{\text{inlet}} = 8$ atm cases to $Z \approx 22$ km for the $p_{\text{inlet}} = 4$ atm cases. This altitude jump not only lowered the drag on the airframe for about the same amount of lift (shown in Figs. 17, 24, and 25 for mass, drag, and L/D, respectively) but allowed for an increase in the fuel mass fraction π_f (Fig. 18).

The increase in π_f for case 4 over case 3 resulted from the inlet needing larger compression ramp angles to generate the required inlet pressure (caused by lower atmospheric pressure at $Z = 22$ km), giving more volume for fuel (Fig. 19) and a higher structural volumetric efficiency (Fig. 20). The height of the vehicle was increased as a result of the larger capture area required to allow enough air mass to enter the engine (shown in Figs. 13, 16, and 21). The combination of larger compression ramp angles and increased cruising altitude caused problems for optimization cases 8 through 10 (i.e., no solutions existed). The two-engine model was already height restricted, and the larger angles caused the height to be too large for a viable geometry to fit within the 0.61-m height constraint. In addition, the two-engine models had problems generating the required lift and propulsive forces at the increased altitude caused by the relative lack of additional capture area and large increase in mass (shown in Figs. 13 and 17). The single-engine model with $\kappa = 30\%$ (case 8) experienced problems at $p_{\text{inlet}} = 4$ atm because the loss of mass created an unresolved pitching moment problem as a result of the excess lift generated by the forebody and the counteracting negative control-surface deflection.

The effects of the large structural mass estimation on the two-engine designs becomes apparent by looking at Figs. 5–7. Figure 5, for case 5, shows that the forebody lift was augmented by the large nozzle surface with negligible control-surface deflection in order to achieve the trim, steady-state cruise optimization conditions. The change from $\kappa = 30\%$ for case 5 to $\kappa = 50\%$ for cases 6 and 7 resulted in considerable control force to achieve a trim condition. This result indicates that the control surface was not just counteracting moment, but generating large amounts of lift (and drag), thus creating false engine and mass capture requirements. Therefore, even though the structural mass estimation was made to suit the single-engine cases, the two-engine cases were substantially penalized. The true benefits of the two-engine configurations will only be realized through improved structural mass estimations.

Conclusions

A methodology and analysis has been presented for design of single- or multiple-engine hypersonic missile designs, which were constrained to fit within a fixed geometric box. Using the outlined design tool, a parametric study has been performed to explore the sensitivities of critical design parameters and to quantify possible upper limits on cruising range achievable through increased modeling accuracy. To this end, the parameters that currently contribute the largest degree of error to this model and that should be resolved are 1) the engine inlet pressure required to complete combustion of a hydrocarbon fuel within the constrained combustor lengths without silane, 2) the structural requirements to complete the current mission, 3) the sizing and arrangement of internal components to allow for the largest amount of fuel, and 4) increased aerodynamic prediction capability. Without more detailed structural modeling, it is still unknown if achieving the desired 750-km goal is possible, but any approach to this limit will only be reached through the ongoing multidisciplinary design optimization studies for this missile geometry.

The most probable design for this missile application will have two engines (at least) but will fall short of the desired 750-km goal unless significant engine improvements are made (mixing and ignition lengths) allowing for a decrease in the inlet pressure. The two-engine designs have much lower sensitivity to the assumed energy recovery from the fuel and should have larger fuel mass fractions when proper subsystems analyses are completed. Increased structural accuracy will favor the two-engine design (requiring less lift), where single-engine designs may have to use some sort of ballast incorporated in the forebody or control surface deflection to balance lift. Improved aerodynamic modeling should lower pressure forces on the aftbody of double-engine designs, thereby lowering the propulsive requirements. These improvements in geometric, aerodynamic, and propulsive modeling are currently being investigated.

Acknowledgments

This research was supported by the Center for Hypersonic Education and Research at the University of Maryland under Technical Monitor Isaiah Blankson of NASA (NASA Grant NAGw 11796), the support of whom is greatly appreciated. Appreciation is also expressed to Timothy O'Brien for the engine model and to Jee Su Chang for the chemical reaction rates (both of the University of Maryland).

References

[1]Nonweiler, T. R. F., "Aerodynamic Problems of Manned Space Vehicles," *Journal of the Royal Aeronautical Society*, Vol. 63, Sept. 1959, pp. 521–528.

[2]Rasmussen, M., *Hypersonic Flow*, 1st ed., Wiley-Interscience, New York, 1994, pp. 100–136.

[3]Takashima, N., and Lewis, M. J., "Navier–Stokes Computation of a Viscous Optimized Waverider," AIAA Paper 92-0305, Jan. 1992.

[4]Sabean, J., Lewis, M. J., Mee, D., and Paull, A., "Performance Study of a Power Law Starbody," *Journal of Spacecraft and Rockets*, Vol. 36, No. 5, 1999, pp. 646–652.

[5]Starkey, R. P., and Lewis, M. J., "Simple Analytical Model for Parameteric Studies of Hypersonic Waveriders," *Journal of Spacecraft and Rockets*, Vol. 36, No. 4, 1999, pp. 516–523.

[6]Anderson, M. B., *Users Manual for IMPROVE Version 2.3—An Optimization Software Package Based on Genetic Algorithms*, Auburn Univ., Auburn, AL, 1996.

[7]Anderson, M. B., Burkhalter, J. E., and Jenkins, R. M., "Missile Aerodynamic Shape Optimization Using Genetic Algorithms," *Journal of Spacecraft and Rockets*, Vol. 37, No. 5, 2000, pp. 663–669.

[8]Kolodziej, P., Bowles, J. V., Brown, J. L., Cornelison, C. J., Lawrence, S. L., Loomis, M. P., Merriam, M. L., Rasky, D. J., Tam, T. C., Wercinski, P. F., Hodapp, A. E., Deese, D. L., Pilcher, M. W., Tucker, R. D., Bogdanoff, D. W., Chapman, G. T., Gage, P. J., Palmer, G. E., Venkatapathy, E., Bowling, D. B., Holt, D. M., and Yates, L. A., "SHARP-L1 Technology Demonstrator Development: An Aerothermodynamic Perspective," AIAA Paper 2000-2688, June 2000.

[9]Gillum, M. J., and Lewis, M. J., "Experimental Results on a Mach 14 Waverider with Blunt Leading Edges," *Journal of Aircraft*, Vol. 34, No. 3, 1997, pp. 296–303.

[10]Tarpley, C., and Lewis, M. J., "Stability and Control of Hypersonic Waverider Vehicles," *Journal of Aircraft*, Vol. 32, No. 4, 1995, pp. 795–803.

[11]Takashima, N., and Lewis, M. J., "Optimization of Waverider-Based Hypersonic Cruise Vehicles with Off-Design Considerations," *Journal of Aircraft*, Vol. 36, No. 1, 1999, pp. 235–245.

[12]Starkey, R. P., and Lewis, M. J., "Analytical Off-Design L/D Analysis for Hypersonic Waveriders with Planar Shocks," *Journal of Spacecraft and Rockets*, Vol. 37, No. 5, 2000, pp. 684–691.

[13]Lewis, M. J., and Chang, J. S., "Joint Jet-A/Silane/Hydrogen Reaction Mechanism," *Journal of Propulsion and Power*, Vol. 16, No. 2, 2000, pp. 365–367.

[14]Shapiro, A. H., *The Dynamics and Thermodynamics of Compressible Fluid Flow*, Vol. 1, McGraw–Hill, New York, 1953.

[15]Anderson, J. D., *Modern Compressible Flow: with Historical Perspective*, McGraw–Hill, New York, 1990, pp. 307–331.

[16]Anderson, J. D., *Hypersonic and High Temperature Gas Dynamics*, McGraw–Hill, New York, 1989, pp. 70–74.

[17]White, F. M., *Viscous Fluid Flow*, 1st ed., McGraw–Hill, New York, 1974, pp. 28, 29, 511.

[18]Goldberg, D. E., *Genetic Algorithms in Search, Optimization, and Machine Learning*, Addison Wesley Longman, Reading, MA, 1989.

[19]Michalewicz, Z., *Genetic Algorithms + Data Structures = Evolution Programs*, Springer-Verlag, New York, 1996.

M. Torres
Associate Editor